Djamila CHERIFI[1], Yahia MILOUD[1], Mohamed MOSTEFAI[1]

Laboratoire Géométrie, Analyse, Contrôle Et Applications, University of Saida, Algeria (1)

doi:10.15199/48.2023.11.12

High Performance of Direct Power Control for a Doubly Fed Induction Generator Based on Adaptive Fuzzy Second Order Sliding Mode Controller in Wind Energy Conversion System

Abstract. *In this paper, adaptive fuzzy second order sliding mode direct power control strategy is applied for a doubly fed induction generator based wind energy generation system. The conventional direct power control with hysteresis regulators has significant active and reactive power ripples at steady-state operation and also the switching frequency varies in a wide range. The proposed direct power control reduces active, reactive and current ripples. It also narrows down the switching frequency variations in induction machine control. The stator active power reference is given through the fuzzy logic MPPT algorithm to extract the maximum of wind power available at the turbine pales. The simulation results show that the proposed direct power control provides significantly improved control performance especially when compared to the conventional direct power control control.*

Streszczenie. *W tym artykule zastosowano adaptacyjną strategię sterowania mocą ślizgową rozmytą drugiego rzędu w dwustronnie zasilanym systemie wytwarzania energii wiatrowej opartym na generatorze indukcyjnym. Konwencjonalna bezpośrednia regulacja mocy z regulatorami histerezy ma znaczne wahania mocy czynnej i biernej podczas pracy w stanie ustalonym, a także częstotliwość przełączania zmienia się w szerokim zakresie. Zaproponowana bezpośrednia regulacja mocy ogranicza tętnienia czynne, bierne i prądowe. Zawęża również zmiany częstotliwości przełączania w sterowaniu maszyną indukcyjną. Wartość odniesienia mocy czynnej stojana jest podawana za pomocą algorytmu MPPT z logiką rozmytą w celu wyodrębnienia maksymalnej mocy wiatru dostępnej na łopatkach turbiny. Wyniki symulacji pokazują, że proponowana bezpośrednia regulacja mocy zapewnia znacznie lepszą wydajność regulacji, zwłaszcza w porównaniu z konwencjonalną bezpośrednią regulacją mocy. (**Wysoka wydajność bezpośredniego sterowania mocą dla podwójnie zasilanego generatora indukcyjnego opartego na adaptacyjnym rozmytym kontrolerze trybu ślizgowego drugiego rzędu w systemie konwersji energii wiatrowe**j)*

Keywords: wind energy conversion system; maximum power point tracking; adaptive fuzzy second order sliding mode controller; direct power control; space vector modulation.
Słowa kluczowe: system konwersji energii wiatrowej; śledzenie maksymalnego punktu mocy; adaptacyjny rozmyty regulator trybu ślizgowego drugiego rzędu; bezpośrednia kontrola mocy; modulacja wektora przestrzeni

Introduction

Today, wind energy has become a viable alternative for energy production, in addition to other renewable energy sources. While the majority of installed wind turbines are at fixed speed, the number of variable speed wind turbines continues to grow, [1], [2]. Currently, the market for wind turbine generators with variable speed has turned to powers greater than 1MW, in particular to make the most of the wind field on the site of implantation, [3].

These generators often use the doubly fed induction generator (DFIG) as a generator because of its advantages, [4]. In fact, the most typical connection diagram of this machine is to connect the stator directly to the network, while the rotor is fed through two static converters in back-to-back mode (one side rotor and the other side network). This last configuration allows operation of the variable speed wind turbine which gives the possibility to produce the maximum possible power over a wide range of speed variation (± 30% around the speed of synchronism), [5]. In addition, the static converters used to control this machine can be sized to let through only a fraction of the total power, [6]. This implies fewer commutative losses, a lower converter production cost and a reduction in the size of the passive filters, thus reducing costs and additional losses, [7].

Wind turbines used for the production of electricity must make it possible to produce maximum power by making the best use of the energy available in the wind. This is why many wind turbine control systems, acting on the mechanical or electrical part, are developed to maximize the energy conversion. This is referred to as Maximum Power Point Tracking (MPPT). It is possible to change the pitch angle of the blades, or the rotational speed of the propeller or even play on the control of the generator, [8], [9], [10].

The search for the maximum power is done permanently and the wind turbine therefore adapts itself to each variation of wind to be in a configuration of maximum extraction of power. Such systems also incorporate safety devices that allow for example to limit the power produced when the wind becomes too high and may damage the wind turbine, [11].

The power converter consists of a rotor-side converter and a grid-side converter in which the rotor-side converter controls the active and reactive power and the grid-side converter controls the DC-link voltage and ensures operation of the converter at a unity power factor. Control of a DFIG is traditionally achieved through control of the components of the voltage vector in a field-oriented control (FOC), which is achieved by a rotor current controller. One main drawback of this system is that its performance depends greatly on accurate machine parameters pertaining to the stator, rotor resistances, and inductances, [12], [13].

Different algorithms have been proposed to improve the conventional vector control of the DFIG system. Nowadays, direct control techniques for the DFIG have found a lot of interests due to their simplicity and high dynamic performances, [14].

In the Direct Torque Control (DTC) of an induction machine, the control strategy is based on the selection of appropriate stator voltage vectors in order to maintain the torque and the stator flux within their hysteresis bands. The direct power control (DPC) is based on the well known a DTC for induction machines. Recently, the DPC is proposed for the control of ac motors and more recently DFIGs. In DPC, the converter switching states are selected from a switching table, based on the error between the reference and estimated values of active and reactive powers and the angular position of the ac voltage or the virtual flux , [14], [15].

Although this technique is simple and robust against parameters variations, but the converter switching frequency widely varies as a function of variations of the active and reactive powers and the hysteresis bandwidth. In order to solve the drawback highlighted above, [16], [17], we will propose a technique that reduces oscillations at power levels by imposing a constant switching frequency. In the latter we replace the switching table with a vector-type modulation (SVM: Space Vector Modulation).

in this work, it is to develop a hybridization between the adaptive fuzzy logic controller and the higher order sliding mode controller. So, we call the controller resulting from this hybridization, Adaptive Fuzzy Second Order Sliding Mode (AFSOSMC) that is used instead of the integral proportional controller (PI) to further improve control performance of the DFIG.also the reference of the stator active power is given in order to extract the maximum of the available wind power at the blades of the turbine while applying the technique MPPT floue.

Wind turbine conversion system

A wind energy conversion system (WECS) is a system full of interconnected components that work together to convert the kinetic energy of wind into mechanical energy and then into electrical energy using generators, [18]. Fig.1 shows the diagram of the wind system.

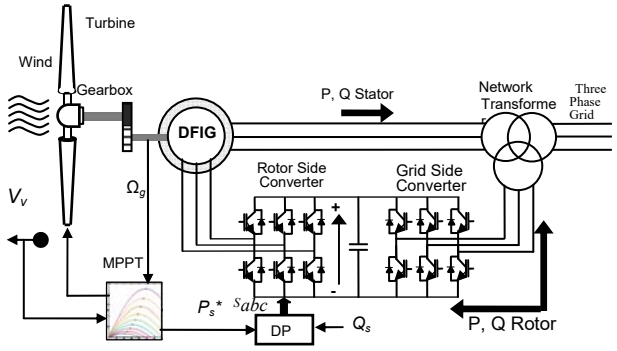

Fig. 1. Wind energy conversion chain

The power given by the wind is as follows, [19]:

$$P_{tur} = C_p \frac{\rho \cdot \mathrm{S} \cdot V_v^3}{2} \quad (1)$$

Where: C_p represents the wind turbine power conversion efficiency. It is a function of the tip speed ratio λ and the blade pitch angle β in a pitch-controlled wind turbine.

λ is defined as the ratio of the tip speed of the turbine blades to wind speed, [19]:

$$\lambda = \frac{R \cdot \Omega_t}{V_v} \quad (2)$$

Where R is blade radius. Ω is angular speed of the turbine. C_p can be described as, [19]:

$$C_p = (0{,}5 - 0{,}0167 \cdot (\beta - 2)) \cdot \sin\left[\frac{\pi(\lambda + 0{,}1)}{18{,}5 - 0{,}3 \cdot (\beta - 2)}\right] - 0{,}0018 \cdot (\lambda - 3)(\beta - 2) \quad (3)$$

The rotor torque is obtained from the power received and the speed of rotation of the turbine, [20]

$$T_t = \frac{P_t}{\Omega_t} = C_p \cdot \frac{\rho \cdot \mathrm{S} \cdot V_v^3}{2 \cdot \Omega_t} \quad (4)$$

The turbine rotational speed is as follows, [20]:

$$\Omega_g = G.\Omega_t \quad (5)$$

The complete dynamic model of the wind system is compiled using the mechanical equation, [20]:

$$T_{mec} - T_{em} = \left(\frac{J_{tur}}{G^2} + J_{gen}\right)\frac{d\Omega_g}{dt} + f_v \cdot \Omega_g \quad (6)$$

MPPT algorithm

Wind turbines used for the production of electricity must make it possible to produce maximum power by making the best use of the energy available in the wind. This is why many control systems of the wind turbine, acting at the mechanical part via the wedge angle of the blades or electric by the control of the electrical machine via the power electronics , are developed to maximize energy conversion, [21],[22], [23].

This control strategy consists of adjusting the electromagnetic torque of the generator so as to set the mechanical rotation speed at a reference speed making it possible to extract the maximum power from the turbine. Thus, a servocontrol of the speed of rotation of the DFIG must be performed, [24] .

For a given operating point (fixed wind speed), the mechanical power is maximum if the maximum value of the coefficient C_p is reached. This is obtained if the relative speed λ is equal to its optimum value λ_{opt} . Therefore, the reference speed of the DFIG Ω_g^* is obtained from Equation (5) as follows :

$$\Omega_g^* = G.\Omega_t \quad (7)$$

With:

$$\Omega_t = \frac{\lambda_{opt} \cdot V_v}{R} \quad (8)$$

The reference electromagnetic torque for having a rotation speed Ω_g equal to its reference value Ω_g^* obtained at the output of the speed regulator.

A fuzzy logic type regulator thus makes it possible to control the speed of rotation and to attenuate the effect of the torque of the DFIG considered as a disturbance.

The schematic diagram of the MPPT control with servo-control of the mechanical speed of rotation is shown in Figure 2.

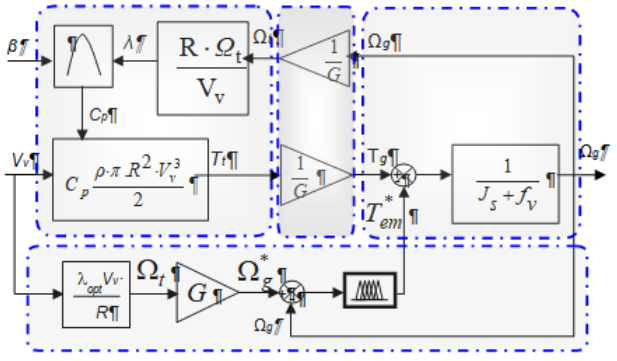

Fig. 2. MPPT control with mechanical speed control

Fuzzy logic MPPT controller

In this paper, the fuzzy logic controller is presented to track the maximum power from the wind by using the rotor speed of the wind.

Fuzzy logic is the best controller to track the maximum power point, [25]. The inputs of the fuzzy controller are the error of speed and change in this error.

The output of the fuzzy controller is the reference torque. At first, the various terms are selected to form the fuzzy rules. Based on these terms, the different rules are formed.
The basic scheme of the fuzzy logic controller is represented as follows:

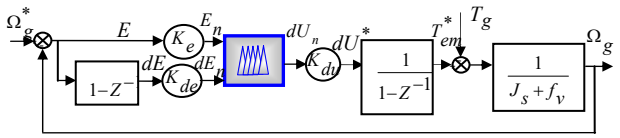

Fig. 3. Fuzzy logic controller structure

E : the error, it is defined by

(9) $$E(k) = \Omega^*(k) - \Omega(k)$$

dE: the derivative of the error, it is approximated by:

(10) $$dE(k) = E(k) - E(k-1)$$

and the control signal is determined by the following relation:

(11) $$U^*(k) - U^*(k-1) + dU^*(k) = T_{em}^*(k)$$

K_e, K_{de}, K_{du} are normalization gains that can be constant (or even variable). The proper choice of these gains allow to guarantee the stability and to improve the dynamic and static performances of the system to be regulated.

The fuzzy rules for determining the output variable of the controller according to input variables are grouped in Table.1

TABLE 1: INFERENCE MATRIX

		E				
		NB	**N**	**EZ**	**P**	**PB**
dE	NB	NB	NB	N	N	EZ
	N	NB	N	N	EZ	PB
	EZ	NB	N	EZ	P	PB
	P	NB	EZ	P	P	PB
	PB	EZ	P	P	PB	PB

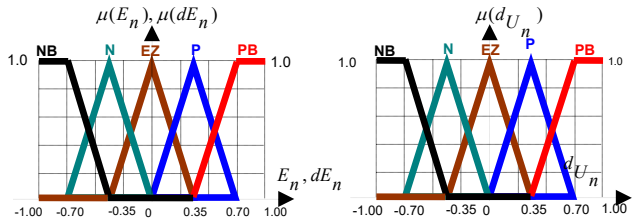

Fig. 4. Membership functions

DFIG Model

The equations of voltages for the DFIG stator and rotor in the Park reference frame are given as follows, [26]:

(7) $$\begin{cases} V_{sd} = R_s i_{sd} + \frac{d}{dt}\phi_{sd} - \omega_s \phi_{sq} \\ V_{sq} = R_s i_{sq} + \frac{d}{dt}\phi_{sq} + \omega_s \phi_{sd} \\ V_{rd} = R_r i_{rd} + \frac{d}{dt}\phi_{rd} - \omega_r \phi_{rq} \\ V_{rq} = R_r i_{rq} + \frac{d}{dt}\phi_{rq} + \omega_r \phi_{rd} \end{cases}$$

Where:

The rotor frequency ω_r is given by:

(8) $$\omega_r = \omega_s - \omega$$

The electromagnetic torque T_{em} is given bys, [27]:

(9) $$T_{em} = \frac{3}{2} p \frac{M}{L_s}\left(\phi_{sq} i_{rd} - \phi_{sd} i_{rq}\right)$$

The active and reactive stator and rotor powers are given by,[19], [28]:

(10) $$\begin{cases} P_s = \frac{3}{2}\left(v_{sd} i_{sd} + v_{sq} i_{sq}\right) \\ Q_s = \frac{3}{2}\left(v_{sq} i_{sd} - v_{sd} i_{sq}\right) \end{cases}$$

(11) $$\begin{cases} P_r = \frac{3}{2}\left(v_{rd} i_{rd} + v_{rq} i_{rq}\right) \\ Q_r = \frac{3}{2}\left(v_{rq} i_{rd} - v_{rd} i_{rq}\right) \end{cases}$$

And the total active and reactive powers of the DFIG are:

(12) $$P = P_s + P_r$$

(13) $$Q = Q_s + Q_r$$

(11)

Where positive values of P and Q mean that the DFIG injects power into, and negative draws power from the grid, [29].

Direct Power Control Strategy

Direct Power Control (DPC) is based on the concept of direct control of the electromagnetic torque (DTC), [30]. The unique difference is the directly controlled variables. In the case of DTC, the electromagnetic torque and the stator flux are directly controlled, while in DPC, the stator active and reactive powers are directly controlled by selecting the optimum switching state of the converter, [31], [32]. Direct Power Control (DPC) was initially proposed by its simplicity, allowing fast power response without the complex field-orientation block. It doesn't require the knowledge of the machine parameters, and due to this, it shows great robustness, [33], [34], [35]. The operating principle of the control is relatively simple with three stages: we have the flux and both active and reactive powers estimation part, then the hysteresis controllers and finally the optimal vector selection table makes it possible to give the necessary signals to control the rotor side converter.

By using previous equations and neglecting the stator resistance, we find the relations of P_s and Q_s according to both components of the rotor flux in the stationary (α_r-β_r) reference frame, and then we can get:

(14) $$\begin{cases} P_s = -\frac{3}{2}\frac{L_m}{\delta L_s L_r} V_s \phi_{r\beta} \\ Q_s = \frac{3}{2}\left(\frac{V_s}{\delta L_s}\phi_s - \frac{L_m}{\delta L_s L_r} V_s \phi_{r\alpha}\right) \end{cases}$$

Where:

(15) $$\begin{cases} \phi_{r\alpha} = \sigma L_r i_{r\alpha} + \frac{L_m}{L_s}\phi_s \\ \phi_{r\beta} = \sigma L_r i_{r\beta} \\ \left|\overline{\phi_s}\right| = \frac{\left|\overline{V_s}\right|}{\omega_s} \\ \sigma = 1 - \frac{L_m^2}{L_s L_r} \end{cases}$$

By introducing the angle δ between the rotor and stator flux linkage, P_s and Q_s become:

$$\begin{cases} P_s = -\dfrac{3}{2}\dfrac{L_m}{\delta L_s L_r}\omega_s |\phi_s||\phi_r|\sin\delta \\ Q_s = \dfrac{3}{2}\dfrac{\omega_s}{\sigma L_s}|\phi_s|\left(\dfrac{L_m}{L_r}|\phi_r|\cos\delta - |\phi_s|\right) \end{cases} \quad (16)$$

The derivative of the two equations in (25) gives:

$$\begin{cases} \dfrac{dP_s}{dt} = -\dfrac{3}{2}\dfrac{L_m}{\delta L_s L_r}\omega_s |\phi_s|\dfrac{d\left(|\phi_r|\sin\delta\right)}{dt} \\ \dfrac{dQ_s}{dt} = \dfrac{3}{2}\dfrac{L_m\omega_s}{\sigma L_s L_r}|\phi_s|\dfrac{d\left(|\phi_r|\cos\delta\right)}{dt} \end{cases} \quad (17)$$

However, the conventional DPC has several drawbacks which make it difficult to be applied in the DFIG-based wind power generation system, [36]. For example, the rotor voltages generated by a fixed and discrete switching table cannot satisfy the control precision of the active and reactive powers during maximum wind energy capturing. Furthermore, the electromagnetic torque vibration caused by the traditional DPC is much more significant than that in the vector control with the same sampling frequency. Moreover, the conventional DPC complicates the AC filter design because of its variable switching frequency. To overcome these drawbacks, several modified DPC strategies have been reported. In this study, in order to obtain a smooth operation at a constant switching frequency, active and reactive power are regulated by two new controllers Adaptive Fuzzy Second Order Slide Mode then a space vector modulation "SVM" algorithm is used to obtain the switching state for the controller.

These modifications make it possible to work at a constant switching frequency which allows to obtain very good dynamics since the current is already limited by the modulator.

Second Order Slide Mode Controller-DPC of the DFIG

The major problem of the classical sliding-mode control is the chattering phenomenon caused by the control switching, which may have undesirable effects on the machine, such as overheating of the windings, torque pulsation, current harmonics, acoustic noise, etc. [37], [38].
The basic idea is to stabilize the dynamics in the small interval in a discontinuous surface without changing the essential characteristics of the whole system. A higher-order sliding-mode is one of the most efficient methods to overcome these problems, [38, 39].
In our case, we consider the surfaces defined by the following equations, [40] :

$$\begin{cases} S_1 = P_s^* - \hat{P}_s \\ S_2 = Q_s^* - \hat{Q}_s \end{cases} \quad (18)$$

With : P_s^* and Q_s^* are successively the references of the active and reactive powers.

The derivative of surfaces is:

$$\begin{cases} \dot{S}_1 = \dot{P}_s^* - \dot{\hat{P}}_s \\ \dot{S}_2 = \dot{Q}_s^* - \dot{\hat{Q}}_s \end{cases} \quad (19)$$

The proposed second order sliding mode active-and reactive-power controllers contains two parts:

$$V_{rd} = v_1 + v_2 \quad (20)$$

With :

$$\begin{cases} v_1 = -k_P \cdot sat\left(S_P / \zeta_p\right) \\ v_2 = -l_P \cdot |S_P|^{\rho} \cdot sat(S_P) \end{cases} \quad (21)$$

$$V_{rq} = w_1 + w_2 \quad (22)$$

With :

$$\begin{cases} w_1 = -k_Q \cdot \left(S_Q / \zeta_Q\right) \\ w_2 = -l_Q \cdot |S_Q|^{\rho} \cdot sat(S_Q) \end{cases} \quad (23)$$

Where: constant gains k_P, l_P and k_Q, l_Q verify the stability conditions and $0 < \rho \le 0.5$, [40]

To improve the SOSM-DPC of the DFIG and decrease significantly the effect caused by chattering, we suggest to use a hybrid approach of second order sliding mode and adaptive fuzzy logic (AFSOSMC).
Therefore, the discontinuous control law of the preceding equations becomes:

$$v_1^{fl} = -k_P^{fl} sat\left(s_P / \xi_P^{fl}\right) \quad (24)$$

With :

$$\begin{cases} k_P^{fl} = \alpha k_P \\ \xi_P^{fl} = \alpha \xi_P \end{cases} \quad (25)$$

$$w_1^{fl} = -k_Q^{fl} sat\left(s_Q / \xi_Q^{fl}\right) \quad (26)$$

With :

$$\begin{cases} k_Q^{fl} = \alpha k_Q \\ \xi_Q^{fl} = \alpha \xi_Q \end{cases} \quad (27)$$

The terms k and ξ are therefore adapted by a fuzzy adapter having two inputs (**ε**) and (**dε**) of three membership functions and an ' α ' output of nine membership functions which are represented in Figures. 5 and 6 respectively.

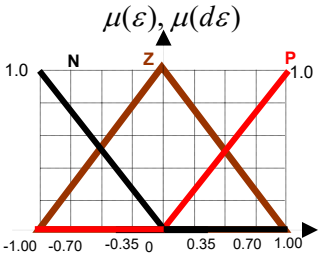

Fig.5. The inputs membership functions of the AFSOSMC controller.

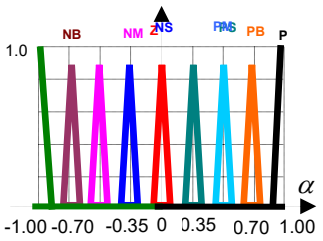

Fig.6. The output membership functions of the AFSOSMC controller.

The linguistic terms used here are represented in Table 2:

Table 2. Linguistic terms

N	Negative	**P**	Positive
Z	Zero	**NB**	Negative Big
NS	Negative Small	**NM**	Negative Medium
PS	Positive Small	**PM**	Positive Medium
PB	Positive Big		

The rules governing the gain adaptation law k and the parameter ξ are given as follows:

R_1 : if S is P and $\dot{S}$ is P Then α is N ;

R_2 : if S is P and $\dot{S}$ is Z Then α is NB ;

R_3 : if S is P and $\dot{S}$ is N Then α is NM ;

R_4 : if S is Z and $\dot{S}$ is P Then α is NS ;

R_5 : if S is Z and $\dot{S}$ is Z Then α is ZE ;

R_6 : if S is Z and $\dot{S}$ is N Then α is PS ;

R_7 : if S is N and $\dot{S}$ is P Then α is PM ;

R_8 : if S is N and $\dot{S}$ is Z Then α is PB ;

R_9 : if S is N and $\dot{S}$ is N Then α is P

Results and Discussion

To investigate the performance of the proposed control strategy under different conditions, extensive simulations are carried out using Matlab/Simulink software. The simulated system is shown in Figure 7 and the system parameters are given in Appendix

MPPT control

Figure 8 shows that a better closed-loop control of the speed is completed under transient and steady state conditions.

A small variation in wind speed introduces a large variation in the power extracted because it is proportional to the cube of the wind speed Fig.9 and we see that the aerodynamic efficiency is almost constant (maximum aerodynamic efficiency) over the whole range of the wind speed Figure 10, by imposing an optimal speed ratio λ_{opt} as shown in Figure 11.

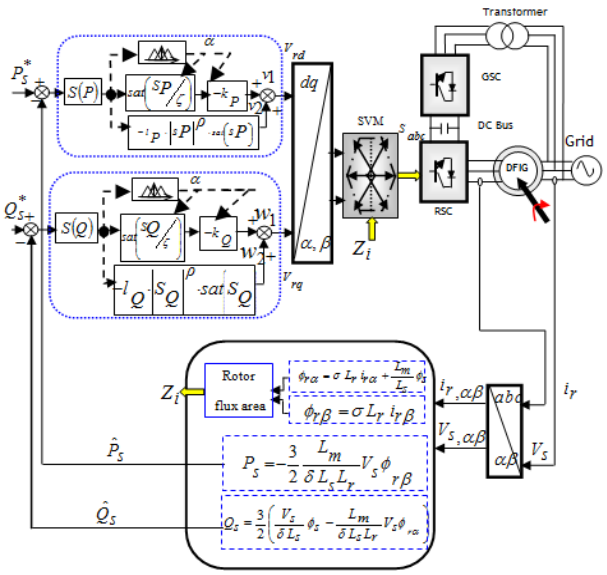

Fig. 7. AFSOSMC_ SVM_ DPC controller scheme

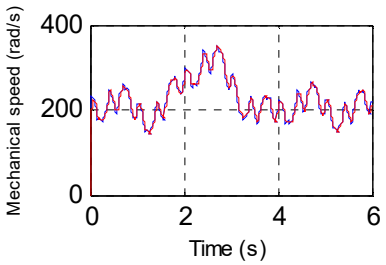

Fig. 8. Speed of turbine

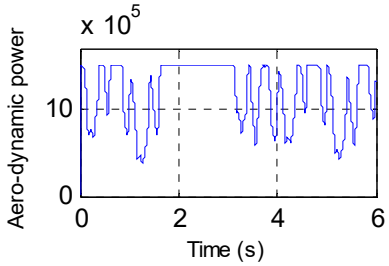

Fig. 9. Aero-dynamic power

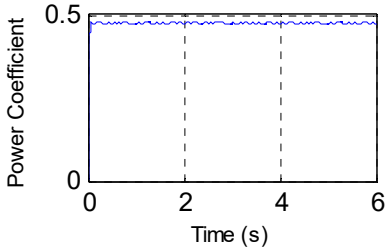

Fig.10. Power coefficient

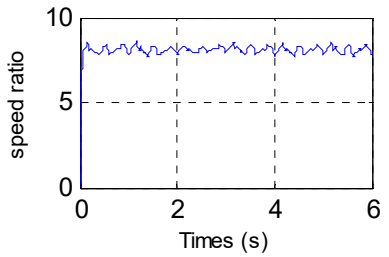

Fig.11. Speed ratio

In the following section, both the AFSOSMC_SVM_DPC and C-DPC controller schemes of the DFIG have been tested by simulation under MATLAB / SIMULINK environment. However, two types of tests were applied to the system of Figure 7 in order to observe the behavior of its regulation:

1- A fixed wind speed (without MPPT control);

2- A variable wind speed (with MPPT control).

MPPT Fixed wind speed (without MPPT control)

In this test, a fixed speed wind of 12m /s is applied to the blades of the wind turbine which corresponds to a hyper synchronous mode of the DFIG. So this first test consists in imposing steps of the active and reactive power, which allows us to verify the decoupling between the two powers of the DFIG Figures 12 and 13.

From the simulation results obtained, it can be said that the decoupling between the active and reactive powers is still achieved but it is also observed from Figure 13 that the AFSOSMC_ SVM_ DPC gives great performance (tracking instructions, time of very fast response, minimal static error ... etc).

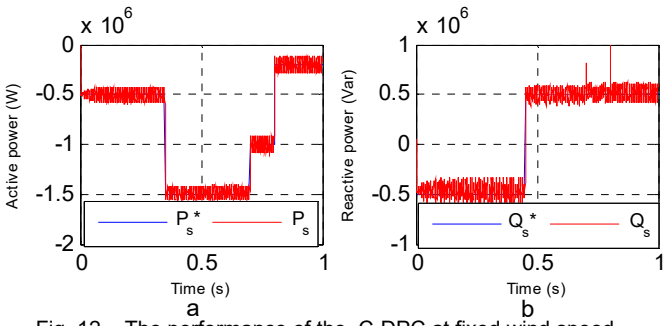

Fig. 12. The performance of the C-DPC at fixed wind speed

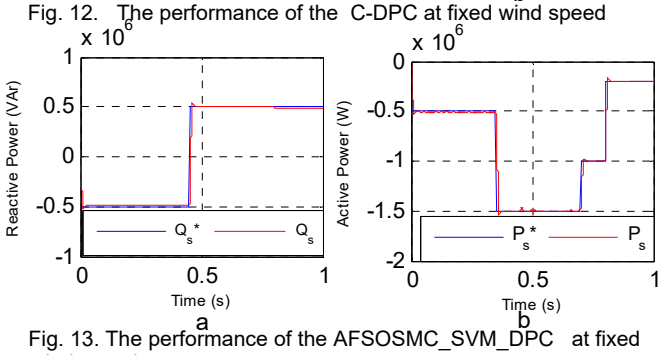

Fig. 13. The performance of the AFSOSMC_SVM_DPC at fixed wind speed

Figure 14 represents the behavior of the DFIG in the case of the C-DPC command, the stator current generated by the DFIG (Figure 14-a) which has a sinusoidal shape but fluctuates because of the variation of the switching frequency (Figure 14-b). The rotor current (Figure 14-c) also seems sinusoidal but still noisy and choppy (Figure 14-d), this is always due to the variable switching frequency of the C-DPC.

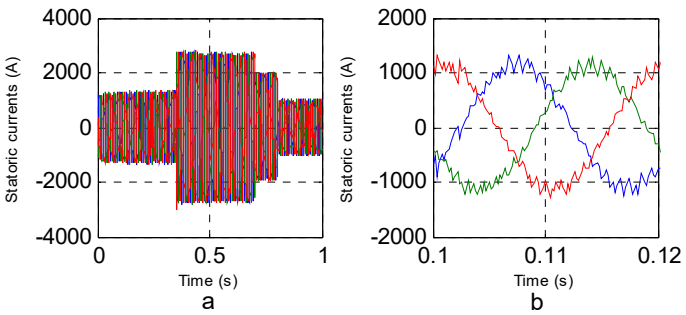

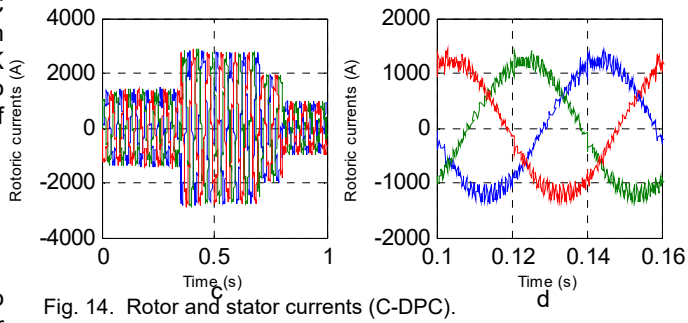

Fig. 14. Rotor and stator currents (C-DPC).

In Fig.15, the behavior of the stator and rotor currents gave us a clear idea about the harmonic rate reduction of the powers and currents injected by the DFIG in the electrical network. These currents have less ripple, with sinusoidal shapes Fig. 15-b and 15-d, this is due to the high performance of the proposed regulation (AFSOSMC) and the fixed switching frequency imposed on the switches by the SVM technique.

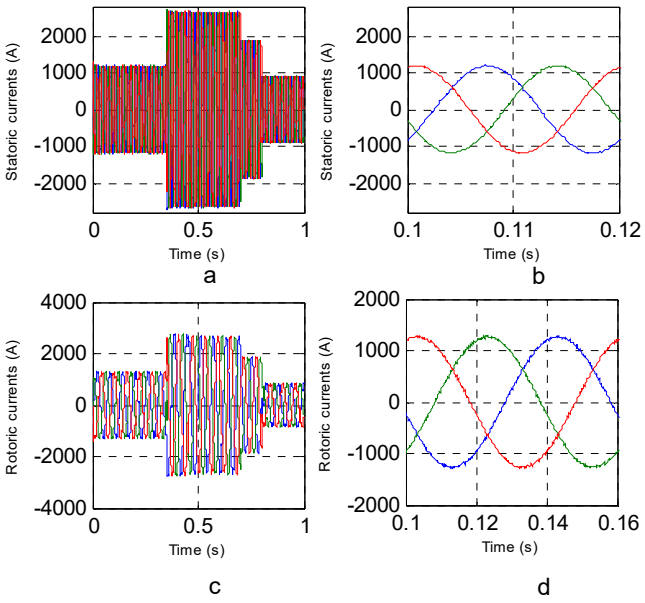

Fig.15. Rotor and stator currents (AFSOSMC_SVM_DPC).

Variable wind speed (with MPPT control)

In the results of the second test (Figs. 16 and 17), the reference value of the reactive power is kept zero (Figs. 16-b and 17-b) in order to ensure a unity power factor on the stator side (Figs. 16-c and 17-c) and to optimize the quality of the energy returned on the network. The setpoint of the active power allows to keep the coefficient of power of the wind turbine optimal whatever the speed of the wind (Fig. 16-a and 17-a); these results are obtained due to the use of the fuzzy logic MPPT technique.

Despite this, the C-DPC technique exhibits strong oscillations (fluctuations) at the levels of the powers. This is mainly due to the variable switching frequency produced by the hysteresis comparators and switching table used by this control technique. These oscillations can cause overheating of the switches.

In Figure 17-a, we observe that the active power follows its reference generated by the MPPT block with a very fast dynamic and we notice that the fluctuations are reduced with respect to the C-DPC (Fig 16-a).

These simulation results show the high performance of the AFSOSMC_ SVM_ DPC developed with the minimization of the pulsations of the powers and the harmonics of the currents presented by the C-DPC command.

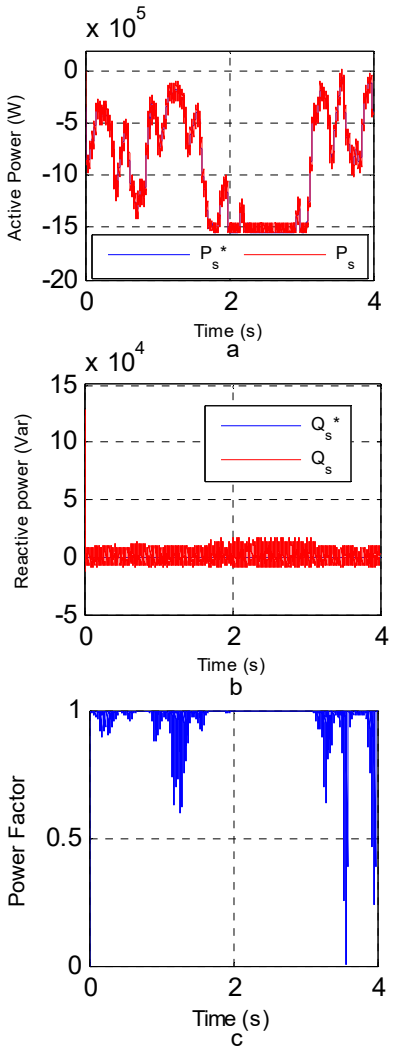

Fig. 16. The performance of the C-DPC at variable wind speed (MPPT Control)

DPC-SVM- AFSOSMC Control Robustness Test

In order to test the robustness of the AFSOSMC_ SVM_ DPC control, we will study the influence of parametric variations (rotor resistance and mutual inductance). This robustness is tested with a simultaneous variation of 100% of the rotor resistance (2×Rr) and 10% of the mutual inductance.

Figures 18 and 19 show the dynamic behavior of the system during this test. The most important quantities are the active and reactive powers. From the results obtained, it can be concluded that the AFSOSMC_ SVM_ DPC has a solid robustness in the presence of the parametric variations of the DFIG

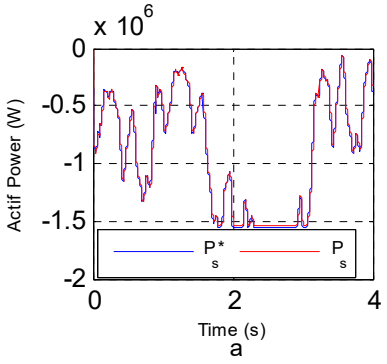

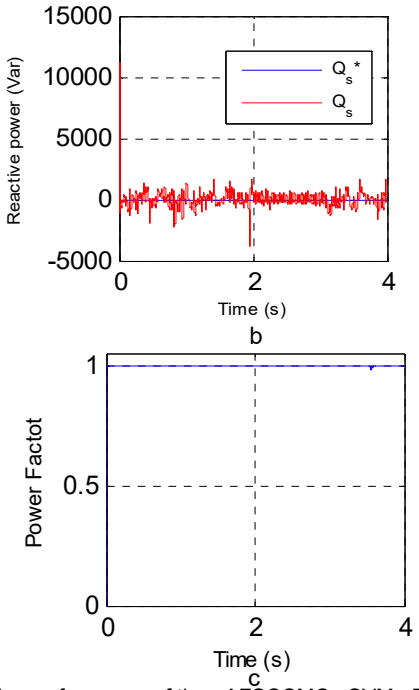

Fig. 17. The performance of the AFSOSMC_ SVM_ DPC at variable wind speed (MPPT Control)

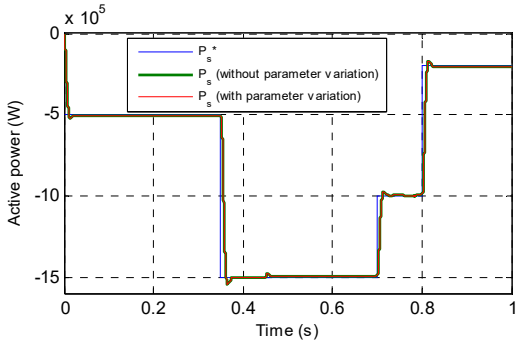

Fig. 18. AFSOSMC_SVM_DPC strategy responses (robustness test).

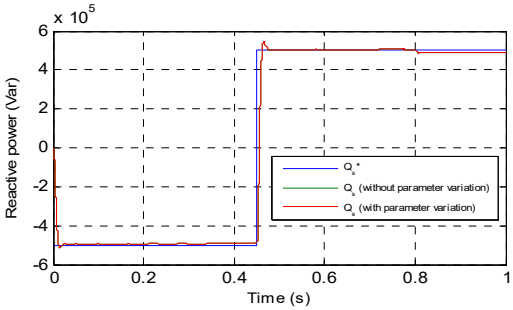

Fig. 19. AFSOSMC_SVM_DPC strategy responses (robustness test).

Conclusion

The objective of this work is the improvement of the quality of the energy supplied to the grid by the DFIG. Hence, a robust SVM_ DPC based on AFSOSMC has been proposed compared to the conventional DPC in terms of tracking instructions, response time, minimum static error and the sinusoidal shape of the currents generated by the DFIG towards the network. The simulation results showed that the combination of the adaptive fuzzy controller and the second-order slip mode resulted in a double advantage: remarkable performance compared to the C-DPC and a significant reduction in the fluctuations of the output quantities of the DFIG and

especially the improvement of the shape of the currents obtained.

APPENDIX: Table 3. Wind Turbine Parameters

Number of blades	3
Blade radius, R	35.25m
Gearbox ratio, G	90
Moment of inertia, J	1000 Kg.m^2
Viscous friction coefficient, f	0.0024N.m.s-1
Cut-in wind speed	4m/s
Cut-out wind speed	25m/s

Table 4. DFIG Parameters

Rated Power Pn	1.5 MW
Stator Voltage Vs	398/690 V
Stator Frequency f	50 Hz
Stator Resistance Rs	0.012 Ω
Rotor Resistance Rr	0.021 Ω
Stator inductance L_s	0.0137 H
Rotor inductance L_r	0.0136 H
Mutual inductance M	0.0135 H
Viscous friction *f*	0.0024 Nm/s
Inertia J	1000 kg m^2
Number of pairs of poles P	2

Authors

Djamila CHERIFI: assist Prof. faculty of Technology University of Moulay Tahar, Saida. Algeria Email:d_cherifi@yahoo.fr.
Miloud Yahia: Prof.Electrical Engineering Institute of The Prof. Faculty of Technology University of Moulay Tahar, Saida. Algeria, Email: miloudyahiadz@yahoo.fr.
Mostefai Mohamed: assist Prof.faculty of Technology University of Moulay Tahar, Saida. Algeria Email:mostefaimed@yahoo.fr

REFERENCES

[1] A. Kassem, K. Hasaneen, and A. Yousef, "Dynamic modeling and robust power control of DFIG driven by wind turbine at infinite grid", Electrical Power and Energy Systems, 2013, pp. 375–382.

[2] H. Ibrahim, M. Ghandour, M. Dimitrova, A. Ilinca, J. Perron, "Integration of Wind Energy into Electricity Systems: Technical Challenges and Actual Solutions", Energy Procedia, 2011, pp. 815–824.

[3] W. Resham, K. Sandeep, S. Rakesh, "Direct active and reactive power control of DFIG for wind energy generation", International Journal of Innovative Research in Electrical, Electronics, Instrumentation and Control Engineering. Vol. 3, Issue 5, May 2015, pp. 138-143.

[4] X. Lie, C. Phillip, "Direct Active and Reactive Power Control of DFIG for Wind Energy Generation", IEEE Transactions on Energy Conversion, VOL. 21, NO. 3, September 2006, pp. 750-758.

[5] Y. Djeriri, A. Meroufel, A. Massoum, Z. Boudjema, A "Comparative Study Between Field Oriented Control Strategy and Direct Power Control Strategy for DFIG", Journal of Electrical Engineering, 2014.

[6] F. Taibi, O. Benzineb, M. Tadjine, M. Boucherit, M. Benbouzid, "Hybrid Sliding Mode Control of DFIG with MPPT Using Three Multicellular Converters", Proceedings of the 19th World Congress The International Federation of Automatic Control Cape Town, South Africa. August 24-29, 2014.

[7] Y. Bekakra, D. Ben Attous, "DFIG sliding mode control fed by back-to-back PWM converter with DC-link voltage control for variable speed wind turbine", Front. Energy, 8(3): 345–354.

[8] J. Thongam, M. Ouhrouche, "MPPT Control Methods in Wind Energy Conversion Systems", Fundamental and Advanced Topics in Wind Power, June 2011, pp. 339-360.

[9] W. Chun, Z. Zhe, Q. Wei, Q. Liyan, "Intelligent Maximum Power Extraction Control for Wind Energy Conversion Systems Based on Online Q-learning with Function Approximation", Energy Conversion Congress and Exposition (ECCE), 2014, pp. 4911-4916.

[10] T. Salma, R. Yokeeswaran, "Pitch Control of DFIG based Wind Energy Conversion System for Maximum Power Point Tracking", International Journal of Advanced Research in Electrical, Electronics and Instrumentation Engineering, Vol. 2, Issue 12, December 2013, pp. 6373-6381.

[11] P. Ghuman, M. Rachna, "Maximum Power Point Tracking in Wind Energy Generation System using DFIG", International Journal of Engineering Trends and Technology (IJETT), Vol.37, N°7, July 2016, pp. 405-407.

[12] A. Nazari, H. Heydari, "Direct Power Control Topologies for DFIG-Based Wind Plants", International Journal of Computer and Electrical Engineering, Vol. 4, No. 4, August 2012, pp. 475-479.

[13] J. Sung-Tak, L. Sol-Bin, P. Yong-Bae, L. Kyo-Beum, "Direct Power Control of a DFIG in Wind Turbines to Improve Dynamic Responses", Journal of Power Electronics, Vol. 9, No. 5, September 2009, pp. 781-790.

[14] M. Pichan, H. Rastegar, M. Monfared, "Two fuzzy-based direct power control strategies for doubly-fed induction generators in wind energy conversion systems", Energy, 2013, pp. 154-162.

[15] D. Kairous, B. Belmadani, "Robust Fuzzy-Second Order Sliding Mode based Direct Power Control for Voltage Source Converter", (IJACSA) International Journal of Advanced Computer Science and Applications, Vol. 6, No. 8, 2015, pp. 167-175.

[16] M. Kazemi, A.S. Yazdankhah, H.M. Kojabadi, "Direct power control of DFIG based on discrete space vector modulation", Elsevier, Renewable Energy, Vol. 35, No. 5, 2010, pp. 1033-1042.

[17] M. Kazemi, M. Moradi, R.V. Kazemi, "Minimization of powers ripple of direct power controlled DFIG by fuzzy controller and improved discrete space vector modulation", Elsevier, Electric Power Systems Research, Vol.89, 2012, pp. 23-30.

[18] Boumerid Bensahila, M. A., Allali, A., Merabet Boulouiha, H., Denai, M. " Modeling, simulation and control of a doubly-fed induction generator for wind energy conversion systems", International Journal of Power Electronics and Drive System (IJPEDS),Vol. 11, No. 3, September 2020, pp. 1197~1210. DOI: 10.11591/ijpeds.v11.i3.pp1197-1210

[19] Vineet, D., Leena, G. " Comparative study of doubly fed induction generator and permanent magnet synchronous generator in wind energy conversion system", International Journal of Electrical Engineering & Technology (IJEET). Volume 10, Issue 3, May-June 2019, pp. 73-79.

[20] Moulay, F., Habbatti, A., Hamdaoui, H. "Application and Control of a Doubly Fed Induction Machine Integrated in Wind Energy System", Instrumentation Mesure Métrologie, Vol. 18, No. 3, June, 2019, pp. 257-265

[21] D. Kumar, K. Chatterjee, "A review of conventional and advanced MPPT algorithms for wind energy systems", Renewable and Sustainable Energy Reviews, 55, 2016, pp. 957-970.

[22] M.A. Abdullah, A.H.M. Yatim, C.W. Tan, R. Saidur, "A review of maximum power point tracking algorithms for wind energy systems", Renewable and Sustainable Energy Reviews, 16, 2012, pp. 3220-3227.

[23] S.M. Raza-Kazmi, H. Goto, "A Novel Algorithm for Fast and Efficient Speed-Sensorless Maximum Power Point Tracking in Wind Energy Conversion Systems", IEEE transactions on industrial electronics, Vol. 58, No. 1, JANUARY 2011, pp. 29-39.

[24] P. Jyothi, B. Mallika, M. Laxman-Rao, "Improve Wind Power Generation by using Servo Motor", International Journal of Advanced Technology and Innovative Research,**Vol.07**, Issue.10, August-2015, pp. 1761-1768.

[25] A. Harrag, S. Messalti, "A variable step size fuzzy MPPT controller improving energy conversion of variable speed DFIG wind turbine", Revue des Energies Renouvelables, Vol. 20 No 2, 2017, pp. 295 - 308.

[26] Chhipa, A. A., Chakrabarti, P., Bolshev, V., Chakrabarti, T., Samarin, G., Vasilyev, A. N., Ghosh, S., Kudryavtsev, A. " Modeling and Control Strategy of Wind Energy Conversion System with Grid-Connected Doubly-Fed Induction Generator", Energies 2022, 15, 6694. https://doi.org/10.3390/en15186694

[27] Benbouhenni, H., Boudjema, Z., Bizon, N., Thounthong, P., Takorabet, N. "Direct Power Control Based on Modified Sliding

Mode Controller for a Variable-Speed Multi-RotorWind Turbine System Using PWM Strategy", Energies **2022**, 15, 3689. https://doi.org/10.3390/ en15103689
[28] Dekali, Z., Lotfi aghli, L., Boumediene, A." Improved Super Twisting Based High Order Direct Power Sliding Mode Control of a Connected DFIG Variable Speed Wind Turbine", Periodica Polytechnica Electrical Engineering and Computer Science, 2021 https://doi.org/10.3311/PPee.17989
[29] R. Yerra-Sreenivasa, A. Jaya-Laxmi, "Direct Torque Control of Doubly Fed Induction Generator Based Wind Turbine Under Voltage DIPS", International Journal of Advances in Engineering & Technology, May 2012, Vol. 3, Issue 2, pp. 711-720.
[30] Y. Djeriri, A. Meroufel, A. Massoum, Z. Boudjema, "Direct power control of a doubly fed induction generator based wind energy conversion systems including a storage unit", Journal of Electrical Engineering, JEE, Romania, 2014, Vol.14, No.1, pp.196-204.
[31] A. Mehdi, A. Reama, H.E. Medouce, S.E. Rezgui, H. Benalla, "Direct Active and Reactive Power Control of DFIG Based Wind Energy Conversion System", International Symposium on Power Electronics, Electrical Drives, Automation and Motion, 2014, pp. 1128-1133.
[32] M.I. Zandzadeh, A. Vahedi, A. Zohoori, "A Novel Direct Power Control Strategy for Integrated DFIG/Active Filter System", 20th Iranian Conference on Electrical Engineering, (ICEE2012), May 15-17, Tehran, Iran, 2012, pp. 564-569.
[33] S.Y. Liu, V.F. Mendese, S.R. Silva, "Analysis of direct power control strategies applied to doubly fed induction generator", XI Brazilian Power electronics conference, IEEE, 2011, pp. 949-954.
[34] M.M. Baggu, L.D. Watson, J.W. Kimball, B.H. Chowdhury, "Direct Power Control of Doubly-Fed Generator Based Wind Turbine Converters to Improve Low Voltage Ride-Through during System Imbalance", twenty-fifth annual IEEE applied power Electronics conference and exposition (APEC), 2010, pp. 2121-2125.
[35] A. Daoud, F. Ben-Salem, "Direct Power Control of a Doubly Fed Induction Generator Dedicated to Wind Energy Conversions", IEEE, 2014, pp.1-8.
[36] F. Amrane, A. Chaiba, S. Mekhilef, "High performances of Grid-connected DFIG based on Direct Power Control with Fixed Switching Frequency via MPPT Strategy using MRAC and Neuro-Fuzzy Control", Journal of Power Technologies, Vol 96. No 1, 2016, pp. 27–39.
[37] P.K. Dash, R.K. Patnaik, "Adaptive second order sliding mode control of doubly fed induction generator in wind energy conversion system", Journal of Renewable and Sustainable Energy, 2014, pp. 1-19.
[38] A. Bouyekni, R. Taleb, Z. Boudjema, K. Kahal, "A second-order continuous sliding mode based on DPC for wind-turbine-driven DFIG", ELEKTROTEHNIŠKI VESTNIK, 85(1-2), 2018, pp. 29-36.
[39] B. Beltran, M.H. benbouzid, A.T. Ahmed, "Second-Order Sliding Mode Control of a Doubly Fed Induction Generator Driven Wind Turbine", IEEE transactions on energy conversion, Vol. 27, NO. 2, JUNE 2012, pp. 261-269.
[40] S. Benelghali, M. Benbouzid, J.F. Charpentier, T. Ahmed-Ali, L. Munteanu, "High-Order Sliding Mode Control of a Marine Current Turbine Driven Permanent Magnet Synchronous Generator", IEEE, 2009, pp. 1541-1546.